

ESVIO: Event-based Stereo Visual Inertial Odometry

Peiyu Chen*, Weipeng Guan*, Peng Lu

Abstract—Event cameras that asynchronously output low-latency event streams provide great opportunities for state estimation under challenging situations. Despite event-based visual odometry having been extensively studied in recent years, most of them are based on the monocular, while few research on stereo event vision. In this paper, we present ESVIO, the first event-based stereo visual-inertial odometry, which leverages the complementary advantages of event streams, standard images, and inertial measurements. Our proposed pipeline includes the ESIO (purely event-based) and ESVIO (event with image-aided), which achieves spatial and temporal associations between consecutive stereo event streams. A well-designed back-end tightly-coupled fused the multi-sensor measurement to obtain robust state estimation. We validate that both ESIO and ESVIO have superior performance compared with other image-based and event-based baseline methods on public and self-collected datasets. Furthermore, we use our pipeline to perform onboard quadrotor flights under low-light environments. Autonomous driving data sequences and real-world large-scale experiments are also conducted to demonstrate long-term effectiveness. We highlight that this work is a real-time, accurate system that is aimed at robust state estimation under challenging environments.

Index Terms—Visual-Inertial SLAM, sensor fusion, aerial systems: perception and autonomy.

MULTIMEDIA MATERIAL

Website: https://github.com/arclab-hku/Event_based_VO-VIO-SLAM.

Video Demo: <https://b23.tv/V23SVzC>.

Code Link: <https://github.com/arclab-hku/ESVIO>.

I. INTRODUCTION

EVENT cameras are novel bio-inspired sensors [1], which have a high dynamic range (140 dB compared to 60 dB of standard cameras) to handle broad illumination conditions. Unlike standard cameras that output fixed-rate image frames, event cameras respond to pixel-level intensity changes and output asynchronous event streams at the latency of microsecond level, which endows these novel sensors to tackle high-speed motion without motion blur.

Most of the existing event-based visual odometers (VO) use monocular event camera [2]–[4], while few research on visual odometry based on stereo event cameras [5] [6]. Since event cameras output asynchronous event streams rather than fixed-rate image frames, the traditional image-based instantaneous matching cannot be directly implemented on event streams. For consecutive stereo event streams, merely

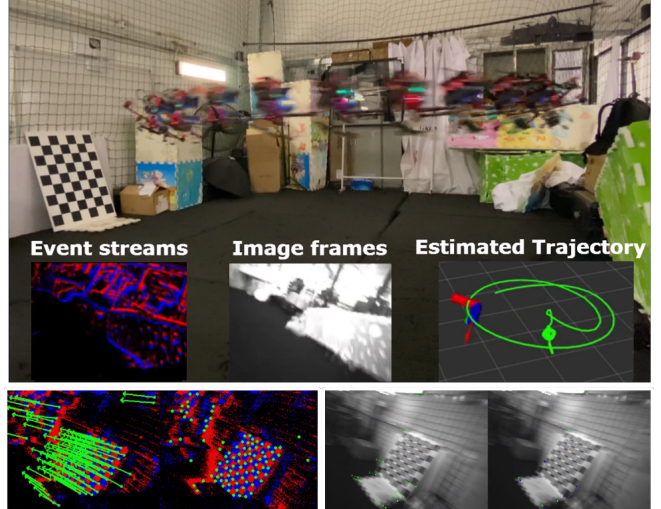


Fig. 1. Our ESVIO provides robust and accurate, real-time pose feedback for drones under aggressive motion. Events provide rich and reliable features, while only a few features are tracked in image frames in high-speed motion. **Left bottom:** stereo event-based feature tracking. **Right bottom:** stereo image-based feature tracking.

relying on temporal constraints to extract and match event-corner features might lead to many false correspondences. Temporal deviations between event streams, noise impacts, different contrast sensitivity of sensors, etc. cause the above problem. Therefore, it is crucial to extract apposite event-corner features and design proper constraints to achieve data association between stereo event-corner features.

Compared with standard cameras, event cameras do not suffer from motion blur under aggressive motion. However, when the relative motion between event cameras and scenes is restricted, e.g. in the stationary state, event streams might not be reliably generated and transmitted, whereas standard cameras are able to provide rich information most of the time (e.g. low-speed motion and well-lit scenes). Observing this complementarity, leveraging both of the advantages of the aforementioned different sensors in combination with an inertial measurement unit (IMU) results in a robust and accurate visual-inertial odometry (VIO) pipeline [3] [4].

In this paper, we propose, to the best of our knowledge, the first published event-based stereo visual-inertial odometry (ESVIO). Our contributions are summarized as follows:

- 1) In order to achieve robust state estimation under aggressive motion and low-light scenarios, we propose the first purely event-based stereo VIO (ESIO) pipeline with sliding windows graph-based optimization, and further extend it with image-aided (ESVIO) which

* Equal contribution.

The authors are with the Adaptive Robotic Controls Lab (ArcLab), Department of Mechanical Engineering, The University of Hong Kong, Hong Kong SAR, China. lupeng@hku.hk.

This research is supported by General Research Fund under Grant No. 17204222, the Seed Funding for Strategic Interdisciplinary Research Scheme and Platform Technology Fund.

tightly integrates stereo event streams, stereo image frames, and IMU together.

- 2) To tackle the problem of event-based stereo feature tracking and matching, we design geometry-based spatial and temporal data associations in consecutive stereo event streams. The spatial and temporal constraints ensure accurate and reliable state estimation. Moreover, a motion compensation method is designed to emphasize the edge of scenes by warping each event.
- 3) We evaluate that our ESVIO can achieve state-of-the-art performance on publicly available datasets. We also release a very challenging event-based VO/VIO dataset, featuring aggressive motion and HDR scenarios. Finally, we perform onboard closed-loop quadrotor flight using our ESVIO as the estimator.

The remainder of the paper is organized as follows: Section II introduces the related works. Section III introduces the methodology of our methods. Section IV presents the experiments and results. Finally, the conclusion is given in Section V.

II. RELATED WORKS

A. Event-based Monocular Visual Odometry

Event-based monocular VO has been intensively researched for challenging scenarios in recent years. [7] is the first work using feature tracks to achieve event-based VO, which detects features firstly from grayscale frames and then uses event streams tracked features asynchronously. EVO [2] proposed a monocular event-based parallel tracking-and-mapping philosophy which applies the image-to-model alignment for tracking and Event-based Multi-View Stereo (EMVS) [8] for mapping. [9] proposed the first event-based VIO that tackles the incomplete estimation of scale and provides accurate 6-DoF state estimation based on Extended Kalman Filter (EKF). [10] obtains a discrete number of states based on a spatio-temporal window of event streams, and introduces virtual event frames to achieve nonlinear optimization that refines estimated poses. Ultimate SLAM [3] furthered the aforementioned research by combining event streams, image frames, and IMU measurements with nonlinear optimization, which leverages the complementary advantages of event cameras and standard cameras. [11] adopted a continuous-time framework based on cubic spline for smooth trajectory estimation and fused both event streams and IMU together. DEVO [12] proposed a novel VO based on a hybrid setup of depth and event cameras, which construct a semi-dense depth map by thresholding time-surface maps. EKLT-VIO [13] integrated an accurate state-of-the-art event-based feature tracker EKLT [14] with EKF backend to achieve event-based state estimation on Mars-like datasets. [15] proposed a real-time monocular event-based VIO based on graph optimization, which directly utilizes the asynchronous raw events for feature detection. PL-EVIO [4] extended the above method to leverage the complementary advantages of standard and event cameras,

which tightly combined event-based point features, event-based line features, image-based point features, and IMU measurements together.

B. Event-based Stereo Visual Odometry

In contrast to monocular VO, which requires sufficient parallax to recover the depth of corner features, stereo VO can directly obtain the depth of features at the current timestamp. This solves scale uncertainty and even tracking failure caused by insufficient parallax. However, most of the recent research on stereo event cameras has focused on depth estimation and constructing semi-dense or dense maps [16] [17], with less research on VO/SLAM fields. ESVO [5] proposed the first event-based stereo VO pipeline, which achieves parallel 3D semi-dense mapping thread and tracking thread by maximizing the spatio-temporal consistency of stereo event streams. [6] adopted stereo feature detection and matching with the geometry method, which adopts reprojection error minimization to achieve pose estimation. However, these algorithms merely use events to estimate the state, which might result in tracking failure when the system is stationary. In addition, these aforementioned approaches without combining IMU might lead to losses of visual tracks under textureless areas. Our work fills a gap based on combining stereo event streams, stereo image frames, and IMU together, which can operate in real-time under high-resolution event streams with better performance than previously proposed methods.

III. METHODOLOGY

Since the procedure of the image measurement is very similar to that of event streams, we only introduce the ESIO in this section. The core of our framework lies in the pre-processing of raw event streams using motion compensation (Section III-A) and the data association between consecutive stereo event streams in temporal and spatial (Section III-B). After that, we design the event-based constraint for graph optimization (Section III-C). The pipeline of ESIO can be represented by the ESVIO (shown in Fig. 2) without image-based processing.

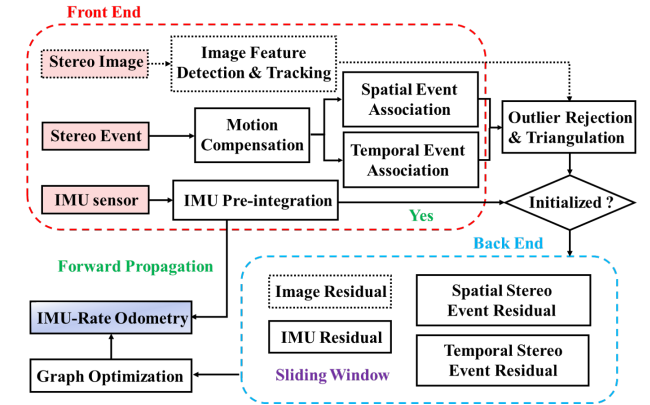


Fig. 2. The structure of our ESVIO and ESIO pipeline.

A. Motion Compensation for Event Streams

Motion compensation corrects the curved event streams by aligning events corresponding to the same scene edge. [18] only uses the angular velocity of IMU to achieve rotational compensation while ignoring the effect of translation. [19] achieve the rotational and translational compensation by IMU and depth camera respectively. We design a motion compensation approach to correct each raw event position, which uses the angular velocity from the IMU sensor and the linear velocity from our ESVIO back-end to achieve rotational and translational compensation respectively. Since our motion compensation utilizes the estimated velocity from the back-end, it works after the successful initialization.

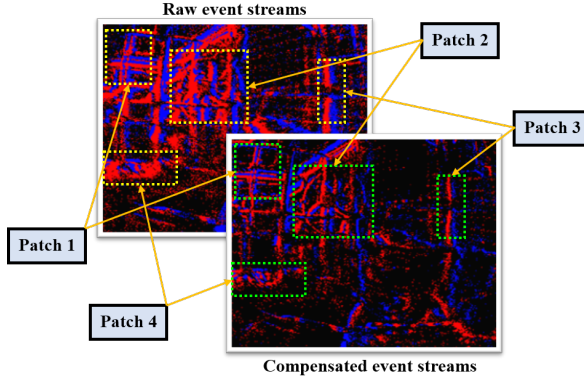


Fig. 3. The event streams without and with motion compensation.

Given the k th event as $e_k = \{l_k, t_k, p_k\}$, where $l_k = \{x_k, y_k\}$ represents the pixel location of the event e_k . t_k is the timestamp and p_k represents its polarity. The event e_k is warped from t_k to t_{ref} , and the compensated location ${}^{ref}l_k$ define as

$${}^{ref}l_k = \mathcal{M}[x_k, y_k, t_k, \Theta] \quad (1)$$

where \mathcal{M} is the motion compensation function. Θ represents compensation parameters. Since the short time interval Δt between t_{ref} and t_k , we assume that the motion during this period is uniform motion, thereby the ego-motion estimation of each event can be formulated as follow:

$$\begin{aligned} {}^{ref}\mathbf{R}_k &= \exp((\tilde{\omega}_k - \mathbf{b}_g(t_k) - \mathbf{n}_g(t_k))\Delta t) \\ {}^{ref}\mathbf{L}_k &= {}^{ref}\mathbf{R}_k \mathbf{L}_k + \mathbf{v}_{ref} \Delta t \end{aligned} \quad (2)$$

where **exp** denotes the exponential map $se(3) \rightarrow SE(3)$. ${}^{ref}\mathbf{R}_k$ is the rotation matrix converted from the Euler angle $\omega_k \Delta t$, $\omega_k = \tilde{\omega}_k - \mathbf{b}_g(t_k) - \mathbf{n}_g(t_k)$. $\tilde{\omega}_k$ is the measurement of gyroscope, while $\mathbf{b}_g(t_k)$ and $\mathbf{n}_g(t_k)$ are bias and noise variable of gyroscope respectively. $\mathbf{L}_k = \{x_k, y_k, 1\}$ is homogeneous matrix that extended from l_k . \mathbf{v}_{ref} represents the velocity of our ESVIO back-end at t_{ref} timestamp. Finally, we convert ${}^{ref}\mathbf{L}_k$ to homogeneous matrix and obtain the compensated location ${}^{ref}l_k$. Fig. 3 compares raw event streams and motion-compensated event streams, where raw event streams produce a certain extent of distortion while the compensated event streams show clear contours of scenes.

B. Event-based Spatial and Temporal Data Associations

After the motion compensation, the stereo event streams are fed to generate two (positive and negative) surface-of-active-event (SAE) which store the event pixels and timestamps. For the new arrival event streams, the existing event-corner features are firstly temporally tracked by the LK optical approach [20] and then spatially matched in left and right event streams. The event-corner features that are not successfully tracked and matched in the current timestamp would be discarded immediately. While new event-corner features are extracted on the motion-compensated event streams to maintain a minimum number (100-200) of features in each timestamp. Modified from the publicly available implementation of the Arc* algorithm [21] for event-based corner detection, we extract the event corners on the individual event by leveraging the SAE. We only select those events whose timestamps are within a short interval from that of the current time surface, thereby retaining event-corner features at the dense event streams. To reduce the influence of noisy events, we further apply time surface (TS) with polarity as a mask to filter effective event-corner features, and the TS is converted from the SAE in real time. Meanwhile, TS is also used to distribute adjacent event-corner features uniformly by setting a minimum distance d_{min} value.

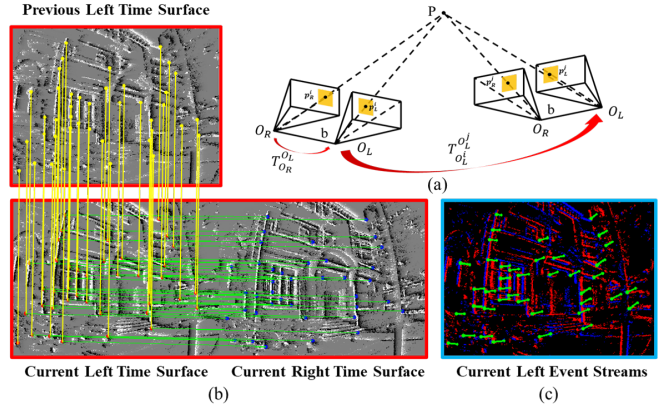


Fig. 4. Stereo event-corner features: (a) Geometry principle; (b) Temporally and spatially associating the event-corner features on the time surface; (c) Event-corner features tracking on the event streams.

The geometry principle of temporal and spatial event-based associations is depicted in Fig. 4(a). To ensure that the matched features between the left and right event streams lie along the epipolar line, we instantaneously match stereo-rectified time surfaces for the spatial association. Stereo event-corner features, \mathcal{F}_L^i and \mathcal{F}_R^i , are instantaneously matched by forward and inverse LK optical flow between the left and right time surface at the current timestamp i . Our ESVIO executes spatial and temporal association at each frame. Meanwhile, the temporal association also uses forward and inverse optical flow to track event-corner features of left event streams, \mathcal{F}_L^i and \mathcal{F}_L^j , at consecutive two timestamps i and j . In Fig. 4(b), red and blue dots represent event-corner features extracted on the left and right

time surface at timestamp i respectively, while yellow dots denote the features on the left time surface at the previous timestamp j . Note that the left bottom and right bottom pictures form the spatial event-based association, while the left bottom and left top pictures form the temporal event-based association. Green lines connect matched event-corner features between the left and right time surfaces at the same timestamp, while yellow lines connect tracked features with two consecutive left time surfaces at i and j . Fig. 4(c) and the bottom of Fig. 1 show our proposed method can achieve correct temporal and spatial association in consecutive stereo event-corner features, even when the image-based tracking is failed caused by the motion blur.

Finally, we recover the inverse depth of event-corner features by RANSAC outlier rejection and triangulation. As depicted in Fig. 4(a), the matched corner features of the 3D point P on the imaging plane of left and right event cameras at timestamp i are p_L^i and p_R^i respectively. The inverse depth of P can be formulated through epipolar geometry and triangulation between p_L^i and p_R^i . Similarly, p_L^i and p_L^j can also be used to recover the inverse depth. Based on these associated event-corner features, corresponding residual constraints can be constructed to conduct graph-based optimization.

C. The Construction of Event-based Residual Constraint for the Graph-based Optimization

The full state vector in the sliding window is defined as

$$\begin{aligned} \mathbf{x} &= [\mathbf{x}_{b_0}, \dots, \mathbf{x}_{b_n}, \mathbf{x}_e^b, \mathbf{x}_c^b, \boldsymbol{\Lambda}_{es}, \boldsymbol{\Lambda}_{et}, \boldsymbol{\Lambda}_c] \\ \mathbf{x}_{b_k} &= [\mathbf{p}_{b_k}^w, \mathbf{q}_{b_k}^w, \mathbf{v}_{b_k}^w, \mathbf{b}_{a_k}, \mathbf{b}_{g_k}] \quad k \in [0, n] \end{aligned} \quad (3)$$

where \mathbf{x}_{b_k} is the state of IMU at timestamp k in the world frame, which consists of the position $\mathbf{p}_{b_k}^w$, the orientation quaternion $\mathbf{q}_{b_k}^w$, the velocity $\mathbf{v}_{b_k}^w$, the accelerometer bias \mathbf{b}_{a_k} and the gyroscope bias \mathbf{b}_{g_k} . \mathbf{x}_e^b and \mathbf{x}_c^b are the extrinsic transformation from event cameras and standard cameras to IMU respectively. $\boldsymbol{\Lambda}_{es} = [\lambda_{es_0}, \lambda_{es_1}, \dots, \lambda_{es_l}]$, $\boldsymbol{\Lambda}_{et} = [\lambda_{et_0}, \lambda_{et_1}, \dots, \lambda_{et_l}]$, $\lambda_{es_l}, \lambda_{et_l}$ represent the inverse depth of the event-corner features es_l , et_l respectively. $\boldsymbol{\Lambda}_c = [\lambda_{c_0}, \lambda_{c_1}, \dots, \lambda_{c_l}]$, λ_{c_l} is the inverse depth of the image-based features c_l . n is the total number of keyframes, and l is the total number of features in the sliding window.

Combining event, image, and IMU residual terms, the event-visual-inertial odometry can be formulated as the joint nonlinear optimization problem as follow

$$\begin{aligned} \min_{\chi} \left(\sum_{k \in b} \left\| \mathbf{r}_b(\hat{\mathbf{z}}_{b_{k+1}}^{b_k}, \chi) \right\|_{\Omega_b}^2 + \sum_{(l,k) \in es} \left\| \mathbf{r}_{es}(\hat{\mathbf{z}}_{es_k}^l, \chi) \right\|_{\Omega_{es}}^2 \right. \\ \left. + \sum_{(l,k) \in et} \left\| \mathbf{r}_{et}(\hat{\mathbf{z}}_{et_k}^l, \chi) \right\|_{\Omega_{et}}^2 + \sum_{(l,k) \in c} \left\| \mathbf{r}_c(\hat{\mathbf{z}}_{c_k}^l, \chi) \right\|_{\Omega_c}^2 \right) \end{aligned} \quad (4)$$

where $\mathbf{r}_b(\hat{\mathbf{z}}_{b_{k+1}}^{b_k}, \chi)$ is the residual for IMU measurement with information matrix Ω_b . $\mathbf{r}_{es}(\hat{\mathbf{z}}_{es_k}^l, \chi)$ and $\mathbf{r}_{et}(\hat{\mathbf{z}}_{et_k}^l, \chi)$ are

the residuals for event-based spatial and temporal association measurement, with corresponding information matrix Ω_{es} and Ω_{et} respectively. $\mathbf{r}_c(\hat{\mathbf{z}}_{c_k}^l, \chi)$ represents the residuals for standard cameras measurement with information matrix Ω_c . The definition of event-based residuals will be presented below, while other residual terms can be found in [4] [22].

For the stereo event cameras, we construct the spatial association factor $\mathbf{r}_{es}(\hat{\mathbf{z}}_{es_k}^l, \chi)$ in the consecutive event streams and the temporal association factor $\mathbf{r}_{et}(\hat{\mathbf{z}}_{et_k}^l, \chi)$ between the left and right event streams. Consider the l th feature that is observed in the i th right event stream, the residual for the event-corner feature observation in the i th left event stream is defined as:

$$\mathbf{r}_{es} = \begin{bmatrix} u_{les_i}^l \\ v_{les_i}^l \end{bmatrix} - \pi_e \left(\mathbf{T}_{re}^{le} \pi_e^{-1} \left(\frac{1}{\lambda_{es}}, \begin{bmatrix} u_{res_i}^l \\ v_{res_i}^l \end{bmatrix} \right) \right) \quad (5)$$

where $[u_{les_i}^l, v_{les_i}^l]$ is the observation of the l th event-corner feature in the i th left event stream. $[u_{res_i}^l, v_{res_i}^l]$ is the same event-corner feature in the i th right event stream. π_e and π_e^{-1} are the projection and back-projection functions of the event camera respectively. \mathbf{T}_{re}^{le} represents the extrinsic transformation from the right to left event camera.

Consider the l th feature that is first observed in the i th left event stream, the residual for the event-corner feature observation in the k th left event stream is defined as:

$$\mathbf{r}_{et} = \begin{bmatrix} u_{et_k}^l \\ v_{et_k}^l \end{bmatrix} - \pi_e \left((\mathbf{T}_{le}^b)^{-1} \mathbf{T}_w^{b_k} \mathbf{T}_{b_i}^w \mathbf{T}_{le}^b \pi_e^{-1} \left(\frac{1}{\lambda_{et}}, \begin{bmatrix} u_{et_i}^l \\ v_{et_i}^l \end{bmatrix} \right) \right) \quad (6)$$

where $[u_{et_k}^l, v_{et_k}^l]$ is the observation of the l th event-corner feature in the k th event stream. $[u_{et_i}^l, v_{et_i}^l]$ is the same event-corner feature in the i th event stream. \mathbf{T}_{le}^b represents the extrinsic transformation from the left event camera to the body coordinate. $\mathbf{T}_{b_i}^w$ indicates the pose of the body center related to the world frame at timestamp i , $\mathbf{T}_w^{b_k}$ is the transpose of the pose of the body coordinate in the world frame at the k th keyframe.

IV. EVALUATION

We perform both dataset and real-world experiments to evaluate our proposed methods. We first evaluate our proposed ESIO and ESVIO in the self-collected dataset which is acquired by two DAVIS346 (346 × 260, event-sensor, image-sensor, IMU sensor) and VICON. It contains extremely fast 6-Dof motion and scenes with HDR. In subsection IV-B, we compare our methods with other event-based and image-based methods on two publicly available datasets: MVSEC [23] and VECtor [24]. We perform quantitative analysis to evaluate the accuracy of our system. The accuracy is measured with mean position error (MPE, %) and mean rotation error (MRE, °/m) aligning the estimated trajectory with ground truth using 6-DOF transformation (in SE3), which is calculated by the tool [25]. Finally, in subsection IV-C we evaluate our ESVIO in the onboard quadrotor flighting. While subsections IV-D1 and IV-D2 perform the evaluation of the autonomous-driving dataset and outdoor

TABLE I. The Accuracy Comparison of Our ESVIO with other Image-based or Event-based Methods on HKU Dataset

Sequence	ORB-SLAM3 [26] Stereo VIO	VINS-Fusion [22] Stereo VIO	USLAM [10] Mono EIO	USLAM [3] Mono EVIO	PL-EVIO [4] Mono EVIO	Our ESIO Stereo EIO	Our ESIO+ Stereo EIO	Our ESVIO Stereo EVIO
	MPE / MRE	MPE / MRE	MPE / MRE	MPE / MRE	MPE / MRE	MPE / MRE	MPE / MRE	MPE / MRE
hku_agg_translation	0.15 / 0.075	0.11 / 0.019	16.22 / 0.45	0.59 / 0.020	0.07 / 0.091	0.59 / 0.16	0.55 / 0.16	0.10 / 0.016
hku_agg_rotation	0.35 / 0.11	1.34 / 0.024	failed	3.14 / 0.026	0.23 / 0.12	1.33 / 0.048	0.78 / 0.045	0.17 / 0.015
hku_agg_flip	0.36 / 0.39	1.16 / 2.02	11.15 / 2.11	6.86 / 2.04	0.39 / 2.23	3.79 / 0.23	3.17 / 0.23	0.36 / 0.12
hku_agg_walk	failed	failed	failed	2.00 / 0.16	0.42 / 0.14	1.49 / 0.23	1.30 / 0.23	0.31 / 0.026
hku_hdr_circle	0.17 / 0.12	5.03 / 0.60	0.92 / 0.58	1.32 / 0.54	0.14 / 0.62	1.38 / 0.10	0.46 / 0.099	0.16 / 0.035
hku_hdr_slow	0.16 / 0.058	0.13 / 0.026	failed	2.80 / 0.099	0.13 / 0.068	0.29 / 0.38	0.31 / 0.39	0.11 / 0.028
hku_hdr_tran_rota	0.30 / 0.042	0.11 / 0.021	failed	2.64 / 0.13	0.10 / 0.064	0.84 / 0.30	0.91 / 0.31	0.10 / 0.018
hku_hdr_agg	0.29 / 0.085	1.21 / 0.27	failed	2.47 / 0.27	0.14 / 0.30	2.33 / 0.16	1.41 / 0.14	0.10 / 0.021
hku_dark_normal	failed	0.86 / 0.028	failed	2.17 / 0.031	1.35 / 0.081	0.30 / 0.12	0.35 / 0.12	0.42 / 0.015
Average	0.16 / 0.12	0.76 / 0.38	5.06 / 1.05	1.69 / 0.39	0.26 / 0.41	0.89 / 0.19	0.66 / 0.19	0.14 / 0.033

*EIO means purely event-based VIO, EVIO means event-based VIO with image-aided

large-scale environment, respectively. All experiments run in real-time on an Intel NUC computer equipped with Intel i7-1260P, 32GB RAM, and Ubuntu 20.04 operation system.

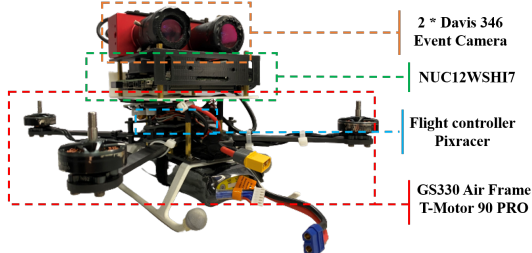


Fig. 5. Our self-designed quadrotor platform.

A. Evaluation of Our ESVIO in Challenging Situations

1) **Experiment Data Description:** The dataset contains stereo event data at 60Hz and stereo image frames at 30Hz with resolution in 346×260 , as well as IMU data at 1000Hz. Timestamps between all sensors are synchronized in hardware. We also provide ground truth poses from a motion capture system VICON at 50Hz for each sequence, which can be used for accuracy comparison. The dataset consists of handheld sequences including rapid motion and HDR scenarios. The full setup including the attached infrared filter can be seen in Fig. 5. These two DAVIS346 are rigidly attached with a baseline of 6.0 cm and USB 3.0 interfaces are used to transmit sensor measurements to the NUC. However, since the limitation of our hardware and cost, we use DAVIS346-COLOR and DAVIS346-MONO for the data collection. Although this might introduce some artificial inconsistency, we think it is acceptable for the method evaluation. The DAVIS comprises an image camera and event camera on the same pixel array, thus calibration can be done using standard image-based methods, such as Kalibr¹, on the image frames and then are applied to the event camera. For the benefit of the research community, we also release the dataset and the configuration files on our project website.

2) **Methods Evaluation:** Table I compares the performance of our ESIO and ESVIO with the other state-of-the-art event-based or image-based systems. Our ESIO has good performance, especially for the sequence *hku_agg_walk* and *hku_dark_normal*, our ESIO still can produce reliable

and accurate pose estimation even when the state-of-the-art image-based VIO method, ORB-SLAM3, fails. Due to motion blur, both ORB-SLAM3 and VINS-Fusion fail to extract reliable features in *hku_agg_walk* sequence, resulting in system failure. In the *hku_dark_normal* sequence, ORB-SLAM3 cannot extract any feature due to poor light conditions (more qualitative details is in the supplementary material). As for the MRE evaluation criterion, our ESVIO shows significant improvement compared to other advanced algorithms, e.g. the average MRE of ESVIO is $0.033^\circ/\text{m}$ while the value of ORB-SLAM3 is $0.12^\circ/\text{m}$. Even if it does not perform too much improvement in MPE compared with our previous work PL-EVIO [4] in most sequences, ESIO and ESVIO are still a breakthrough for event-based stereo VIO. For the motion compensation version (ESIO+), it shows effective improvement in most of the data sequences compared to ESIO, e.g. the average MPE of ESIO+ is 0.66% compared to 0.89% of ESIO, which is opposite to the conclusion from Ref. [4]. This might be thanks to the well-designed motion-compensated methods that process the reliable and optimized compensated measurements from the ESVIO back-end.

Note that we also evaluate EVO [2] and ESVO [5] in our self-collected datasets, but they failed in all sequences. This might be caused by three factors: Firstly, both EVO and ESVO have strict initialization requirements. For example, EVO requires running in a uniform scene for a few seconds to boost the system. Secondly, they are sensitive to parameter tuning, even in their open-source project, they use different parameters for different sequences in the same scenarios. We might fail to correctly tune parameters for their successful running. Finally, our dataset is so challenging that only reliable methods can perform well.

B. Evaluation of Our ESVIO on Public Datasets

In this section, we evaluate our ESVIO on publicly available datasets. The VECToR [24] dataset consists of a hardware-synchronized sensor suite that includes stereo event cameras, stereo standard cameras, an RGB-D sensor, a LiDAR, and an IMU. It covers the full spectrum of 6 DoF motion dynamics, environment complexities, and illumination conditions for both small and large-scale scenarios. To the best of our knowledge, we provide the first results on this

¹<https://github.com/ethz-asl/kalibr>

TABLE II. The Accuracy Comparison of Our ESVIO with other Image-based or Event-based Methods on Public Dataset

Sequence		ORB-SLAM3 [26] Stereo VIO	VINS-Fusion [22] Stereo VIO	EVO [2] Mono EO	ESVIO [5] Stereo EO	Ultimate SLAM [3] Mono EVIO	PL-EVIO [4] Mono EVIO	Our ESVIO Stereo EVIO
		MPE / MRE	MPE / MRE	MPE / MRE	MPE / MRE	MPE / MRE	MPE / MRE	MPE / MRE
VECTOR [24]	corner-slow	1.49 / 14.28	1.61 / 14.06	4.33 / 15.52	4.83 / 20.98	4.83 / 14.42	2.10 / 14.21	1.49 / 14.03
	robot-normal	0.73 / 1.18	0.58 / 1.18	3.25 / 2.00	failed	1.18 / 1.11	0.68 / 1.25	1.08 / 1.17
	robot-fast	0.71 / 0.70	failed	failed	failed	1.65 / 0.56	0.17 / 0.74	0.20 / 0.56
	desk-normal	0.46 / 0.41	0.47 / 0.36	failed	failed	2.24 / 0.56	3.66 / 0.45	0.61 / 0.38
	desk-fast	0.31 / 0.41	0.32 / 0.33	failed	failed	1.08 / 0.38	0.14 / 0.48	0.13 / 0.32
	sofa-normal	0.15 / 0.41	0.13 / 0.40	failed	1.77 / 0.60	5.74 / 0.39	0.19 / 0.46	0.16 / 0.40
	sofa-fast	0.21 / 0.43	0.57 / 0.34	failed	failed	2.54 / 0.36	0.17 / 0.47	0.17 / 0.35
	mountain-normal	0.35 / 1.00	4.05 / 1.05	failed	failed	3.64 / 1.06	4.32 / 0.76	0.59 / 0.77
	mountain-fast	2.11 / 0.64	failed	failed	failed	4.13 / 0.62	0.13 / 0.56	0.16 / 0.45
	hdr-normal	0.64 / 1.20	1.27 / 1.10	failed	failed	5.69 / 1.65	4.02 / 1.52	0.57 / 1.06
	hdr-fast	0.22 / 0.45	0.30 / 0.34	failed	failed	2.61 / 0.34	0.20 / 0.50	0.21 / 0.33
	corridors-dolly	1.03 / 1.37	1.88 / 1.37	failed	failed	failed	1.58 / 1.37	1.13 / 1.33
	corridors-walk	1.32 / 1.31	0.50 / 1.31	failed	failed	failed	0.92 / 1.31	0.43 / 1.32
	school-dolly	0.73 / 1.02	1.42 / 1.06	failed	10.87 / 1.08	failed	2.47 / 0.97	0.42 / 0.73
	school-scooter	0.70 / 0.49	0.52 / 0.61	failed	9.21 / 0.63	6.40 / 0.61	1.30 / 0.54	0.59 / 0.56
	units-dolly	7.64 / 0.41	4.39 / 0.42	failed	failed	failed	5.84 / 0.44	3.43 / 0.022
	units-scooter	6.22 / 0.22	4.92 / 0.24	failed	failed	failed	5.00 / 0.42	2.85 / 0.39
MVSEC [23]	Indoor Flying 1	5.31 / 0.37	1.50 / 0.13	5.09 / 0.92	4.00 / 0.50	failed	1.35 / 0.11	0.94 / 0.14
	Indoor Flying 2	5.65 / 0.41	6.98 / 0.15	failed	3.66 / 0.43	failed	1.00 / 0.16	1.00 / 0.11
	Indoor Flying 3	2.90 / 0.30	0.73 / 0.048	2.58 / 1.25	1.71 / 0.18	failed	0.64 / 0.065	0.47 / 0.043
	Indoor Flying 4	6.99 / 0.79	3.62 / 0.39	failed	failed	2.77 / 0.14	5.31 / 0.23	5.55 / 0.21

new event-based dataset. For the MVSEC [23], we select the sequence captured in the indoor flying room. We use the stereo event camera (640×480) and the regular stereo camera (1224×1024) from the VECToR, and the DAVIS346 (346×260 for both event and image) from the MVSEC, for evaluation, respectively.

As can be seen in Table II, our proposed ESVIO can achieve fairly good results in most of the sequences. Although the MPE criterion of ORB-SLAM3 is slightly better than ours in some sequences (e.g. *robot-normal*, *desk-normal*, *mountain-normal*), our ESVIO provides more reliable and accurate results in most of the sequences under harsh situations with HDR or aggressive motion. The proposed ESVIO is more precise than our previous PL-EVIO, especially in large-scale environments, this might be due to the better event-corner depth estimation. While the traditional event-based methods [2] [3] [5] failed in most of the sequences in these two datasets.

Please note that we think that parameter tuning is infeasible. Therefore, we evaluate our methods using fixed parameters for all sequences during the evaluations. However, the generalization capability of [2] and [5] is slightly poor. Although we have put the utmost effort to tune parameters, they fail in most sequences. Besides, we emphasize real-time performance when evaluating our methods. Table III illustrates the running time of our modules under different resolutions. We also provide a qualitative comparison between our method and the other methods in the accompanying video² and supplementary material.

Last but not the least, although our proposed ESVIO achieves satisfactory results, it still has limitations in the low-texture environment. For example, the scenarios in sequence *units-dolly* and *units-scooter* are so special that the visual-only method might be easy to degenerate or mismatch during

the loop-closure detection. This also indicates that either the event camera or the standard camera has limitations. Although event cameras play a complementary role to the traditional image-based method, event-based multi-sensor fusion, especially combining non-vision-based sensors (such as GPS, and lidar), should be further developed to exploit the advantage of different sensors.

TABLE III. Running time of our modules in different resolution event cameras (ms)

Modules	346 × 260	640 × 480
Motion compensation	2.70	11.11
Creation of event representation	5.12	15.47
Spatial event association	0.82	2.57
Temporal event association	0.83	3.31
The whole process of front-end	10.44	35.69
Back-end optimization	19.30	35.59

C. Indoor Quadrotor Flight Evaluation

To further demonstrate the practicability of our methods, we perform real-world experiments on a self-designed quadrotor platform. We choose Pixracer autopilot as our flight platform with T-Motor F90 PRO, as shown in Fig. 5. The states estimate from our ESVIO is used to provide onboard pose feedback control for the quadrotor. The quadrotor is commanded to follow a circular pattern eight times continuously during the experiment. The robust and accurate onboard state estimates of our ESVIO enable real-time feedback control. Meanwhile, we also record the ground truth from VICON for further quantitative evaluation.

1) **Quadrotor Flight in HDR Scenarios**³: We show the relative pose error (RPE) of our ESVIO against the VICON in Fig. 6(a). The total trajectory length is 56.0m. The boxplot [27] shows that the average relative error for the translation part is around 0.1m. For the rotational part,

²<https://b23.tv/JTkDvCP>

³<https://b23.tv/wcZiKzG>

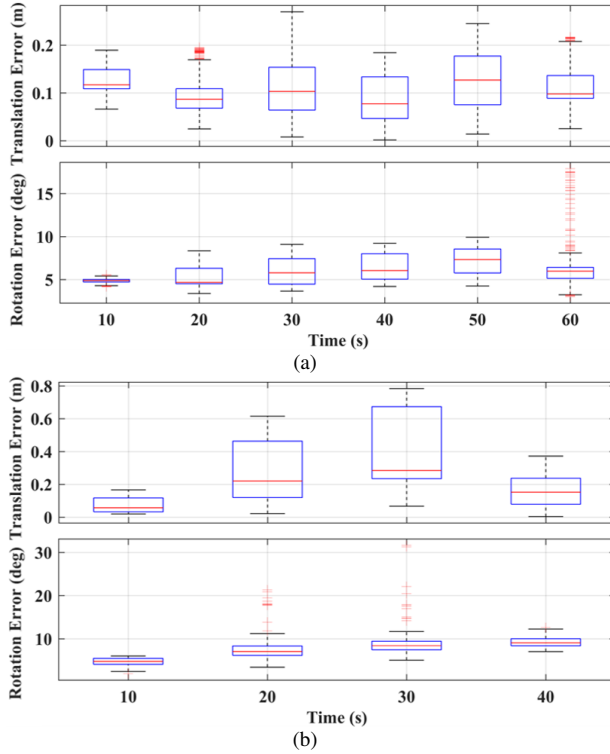


Fig. 6. The relative error comparison of our proposed ESVIO with the VICON: (a) Onboard quadrotor flight in low-illumination conditions; (b) Onboard quadrotor flight in aggressive motion.

the average relative error is around 7° . While there are many outliers from 50 to 60 seconds, which is caused by rapid change in yaw at that moment resulting in the estimated pose being slightly slower than VICON. The root-mean-square error (RMSE) of absolute trajectory error in HDR flight is 0.17m. Fig. 1 qualitatively evaluates the moment when the yaw angle changes rapidly, where few features can be extracted and tracked by the image thread, while event-corner features can still be tracked well.

2) Quadrotor Flight in Aggressive Motion⁴: In this section, the yaw angle of the commanded pattern is changed drastically, for aggressive motion. The performance of our ESVIO is qualitatively demonstrated in Fig. 1 and quantitatively evaluated in Fig. 6(b). The RMSE of ATE in aggressive flight is 0.26m. Note that it would have some outliers during the comparison with the VICON. For example, there are some rotation errors of more than 20° within 20-30 seconds. This is caused by VICON's ball is not well observed during the aggressive flight, resulting in an inaccurate measurement of the VICON at that moment. However, our reliable ESVIO state estimator still provides robust and accurate onboard pose feedback for the quadrotor.

D. Outdoor Large-scale Evaluation

In this section, we evaluate our ESIO and ESVIO in outdoor large-scale environments, including the public-available

⁴<https://b23.tv/nQUbMjy>

autonomous driving dataset and the self-collected HKU campus dataset (More details can be seen on our website).

1) DSEC Dataset: DSEC [28] is collected by high-resolution stereo event cameras (640×480) under driving scenarios, which is challenging for event-based sensors, as forward motions typically produce considerably fewer events at the center. Qualitative evaluation can be seen in Fig. 7. Since the DSEC dataset does not provide the ground truth 6-DoF poses, we only show the estimated trajectory and the tracking performance of our event-based and image-based features. Both our ESIO (available in supplementary material) and ESVIO can achieve satisfactory results.

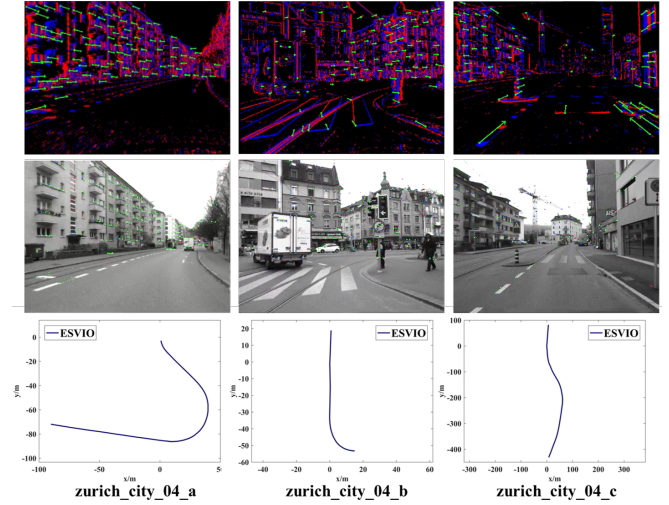


Fig. 7. The qualitative results of ESVIO in DSEC dataset for sequences zurich_city_04 (a) to (c). **Top:** The stereo event-corner feature tracking performance; **Middle:** The stereo image-based feature tracking performance; **Bottom:** The estimated trajectories produced by our ESVIO.

2) HKU Large-scale environment: This section carried out a large-scale experiment on the HKU campus to illustrate the long-time practicability of our ESVIO, features with large-scale, indoor-outdoor conversion, pedestrians in the scene generating outlier events, etc. The path length of the outdoor evaluation is around 1.8 km and the duration is 34.9 minutes. The evaluation covers the place around 310m in length, 170m in width, and 55m in height changes. Since the VICON is not available outdoors, we only show the qualitative performance and the estimated trajectory overlaid with the Google map for visual comparison. As can be seen from Fig. 8, our ESVIO performs well in long-term motion evaluation, the estimated trajectory is aligned and almost coincide with the Google map.

V. CONCLUSIONS

In this paper, we propose a robust, real-time event-based stereo VIO, ESVIO, which tightly fuses the stereo event streams, stereo image frames, and IMU measurements using sliding windows graph-based optimization. Geometry-based spatial and temporal associations between consecutive stereo event streams are designed to ensure robust state estimation.

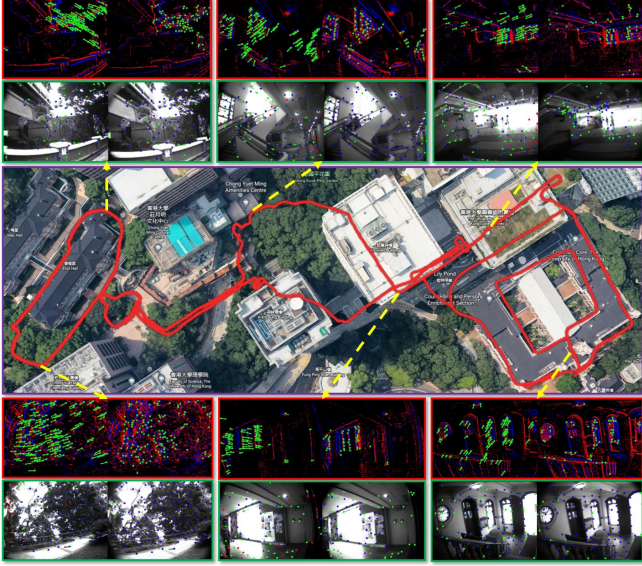


Fig. 8. The estimated trajectory of our ESVIO in the large-scale environment. The detection and tracking situation of the stereo event-corner features and stereo image features during the experiment are also visualized.

In addition, the motion compensation approach corrects the curved event streams with IMU and ESVIO backend to emphasize the contour of scenes. Extensive evaluations demonstrate that our ESVIO achieves superior performance compared to other state-of-the-art algorithms on public datasets and our self-collected challenging datasets. Furthermore, we also perform various onboard closed-loop flights using the proposed ESVIO under low-light scenes and aggressive motion. In our future work, we might further explore the event-based mapping for the quadrotor system which should be able to support autonomous navigation and obstacle avoidance.

REFERENCES

- [1] G. Gallego, T. Delbrück, G. Orchard, C. Bartolozzi, B. Taba, A. Censi, S. Leutenegger, A. J. Davison, J. Conradt, K. Daniilidis, *et al.*, “Event-based vision: A survey,” *IEEE transactions on pattern analysis and machine intelligence*, vol. 44, no. 1, pp. 154–180, 2020.
- [2] H. Rebecq, T. Horstschäfer, G. Gallego, and D. Scaramuzza, “Evo: A geometric approach to event-based 6-dof parallel tracking and mapping in real time,” *IEEE Robotics and Automation Letters*, vol. 2, no. 2, pp. 593–600, 2017.
- [3] A. R. Vidal, H. Rebecq, T. Horstschäfer, and D. Scaramuzza, “Ultimate slam? combining events, images, and imu for robust visual slam in hdr and high-speed scenarios,” *IEEE Robotics and Automation Letters*, vol. 3, no. 2, pp. 994–1001, 2018.
- [4] W. Guan, P. Chen, Y. Xie, and P. Lu, “Pl-evio: Robust monocular event-based visual inertial odometry with point and line features,” *arXiv preprint arXiv:2209.12160*, 2022.
- [5] Y. Zhou, G. Gallego, and S. Shen, “Event-based stereo visual odometry,” *IEEE Transactions on Robotics*, 2021.
- [6] A. Hadviger, I. Cvijić, I. Marković, S. Vražić, and I. Petrović, “Feature-based event stereo visual odometry,” in *2021 European Conference on Mobile Robots (ECMR)*. IEEE, 2021, pp. 1–6.
- [7] B. Kueng, E. Mueggler, G. Gallego, and D. Scaramuzza, “Low-latency visual odometry using event-based feature tracks,” in *2016 IEEE/RSJ International Conference on Intelligent Robots and Systems (IROS)*. IEEE, 2016, pp. 16–23.
- [8] H. Rebecq, G. Gallego, E. Mueggler, and D. Scaramuzza, “Emvs: Event-based multi-view stereo—3d reconstruction with an event camera in real-time,” *International Journal of Computer Vision*, vol. 126, no. 12, pp. 1394–1414, 2018.
- [9] A. Zihao Zhu, N. Atanasov, and K. Daniilidis, “Event-based visual inertial odometry,” in *Proceedings of the IEEE Conference on Computer Vision and Pattern Recognition*, 2017, pp. 5391–5399.
- [10] H. Rebecq, T. Horstschäfer, and D. Scaramuzza, “Real-time visual-inertial odometry for event cameras using keyframe-based nonlinear optimization,” in *British Machine Vision Conference (BMVC)*, 2017.
- [11] E. Mueggler, G. Gallego, H. Rebecq, and D. Scaramuzza, “Continuous-time visual-inertial odometry for event cameras,” *IEEE Transactions on Robotics*, vol. 34, no. 6, pp. 1425–1440, 2018.
- [12] Y. Zuo, J. Yang, J. Chen, X. Wang, Y. Wang, and L. Kneip, “Devo: depth-event camera visual odometry in challenging conditions,” in *2022 International Conference on Robotics and Automation (ICRA)*. IEEE, 2022, pp. 2179–2185.
- [13] F. Mahlknecht, D. Gehrig, J. Nash, F. M. Rockenbauer, B. Morrell, J. Delaune, and D. Scaramuzza, “Exploring event camera-based odometry for planetary robots,” *IEEE Robotics and Automation Letters (RAL)*, 2022.
- [14] D. Gehrig, H. Rebecq, G. Gallego, and D. Scaramuzza, “Eklt: Asynchronous photometric feature tracking using events and frames,” *International Journal of Computer Vision*, vol. 128, no. 3, pp. 601–618, 2020.
- [15] W. Guan and P. Lu, “Monocular event visual inertial odometry based on event-corner using sliding windows graph-based optimization,” in *2022 IEEE/RSJ International Conference on Intelligent Robots and Systems (IROS)*. IEEE, 2022, pp. 2438–2445.
- [16] S. Tulyakov, F. Fleuret, M. Kiefel, P. Gehler, and M. Hirsch, “Learning an event sequence embedding for dense event-based deep stereo,” in *Proceedings of the IEEE/CVF International Conference on Computer Vision*, 2019, pp. 1527–1537.
- [17] Y. Nam, M. Mostafavi, K.-J. Yoon, and J. Choi, “Stereo depth from events cameras: Concentrate and focus on the future,” in *Proceedings of the IEEE/CVF Conference on Computer Vision and Pattern Recognition*, 2022, pp. 6114–6123.
- [18] D. Falanga, K. Kleber, and D. Scaramuzza, “Dynamic obstacle avoidance for quadrotors with event cameras,” *Science Robotics*, vol. 5, no. 40, p. eaaz9712, 2020.
- [19] B. He, H. Li, S. Wu, D. Wang, Z. Zhang, Q. Dong, C. Xu, and F. Gao, “Fast-dynamic-vision: Detection and tracking dynamic objects with event and depth sensing,” in *2021 IEEE/RSJ International Conference on Intelligent Robots and Systems (IROS)*, 2021, pp. 3071–3078.
- [20] B. D. Lucas, T. Kanade, *et al.*, “An iterative image registration technique with an application to stereo vision.” Vancouver, British Columbia, 1981.
- [21] I. Alzugaray and M. Chli, “Asynchronous corner detection and tracking for event cameras in real time,” *IEEE Robotics and Automation Letters*, vol. 3, no. 4, pp. 3177–3184, 2018.
- [22] T. Qin, J. Pan, S. Cao, and S. Shen, “A general optimization-based framework for local odometry estimation with multiple sensors,” *arXiv preprint arXiv:1901.03638*, 2019.
- [23] A. Z. Zhu, D. Thakur, T. Özslan, B. Pfommer, V. Kumar, and K. Daniilidis, “The multivehicle stereo event camera dataset: An event camera dataset for 3d perception,” *IEEE Robotics and Automation Letters*, vol. 3, no. 3, pp. 2032–2039, 2018.
- [24] L. Gao, Y. Liang, J. Yang, S. Wu, C. Wang, J. Chen, and L. Kneip, “Vector: A versatile event-centric benchmark for multi-sensor slam,” *IEEE Robotics and Automation Letters*, 2022.
- [25] M. Grupp, “evo: Python package for the evaluation of odometry and slam,” *Note: https://github.com/MichaelGrupp/evo Cited by: Table*, vol. 7, 2017.
- [26] C. Campos, R. Elvira, J. J. G. Rodríguez, J. M. Montiel, and J. D. Tardós, “Orb-slam3: An accurate open-source library for visual, visual-inertial, and multimap slam,” *IEEE Transactions on Robotics*, 2021.
- [27] Z. Zhang and D. Scaramuzza, “A tutorial on quantitative trajectory evaluation for visual(-inertial) odometry,” in *2018 IEEE/RSJ International Conference on Intelligent Robots and Systems (IROS)*. IEEE, 2018, pp. 7244–7251.
- [28] M. Gehrig, W. Aarents, D. Gehrig, and D. Scaramuzza, “Dsec: A stereo event camera dataset for driving scenarios,” *IEEE Robotics and Automation Letters*, vol. 6, no. 3, pp. 4947–4954, 2021.

Supplementary Materials — ESVIO: Event-based Stereo Visual Inertial Odometry

Abstract

The structure of this document is organized as follows: Section I introduces our self-collected dataset on the HKU campus. Section II supplementarily demonstrates the quantitative performance of our ESIO and ESVIO in the evaluation of rosbag and onboard quadrotor flight. Section III supplementarily demonstrates the qualitative performance of our ESIO and ESVIO in the DSEC dataset; the failure cases of ORB-SLAM3, VINS-Fusion, Ultimate SLAM in our self-collect dataset; The limitations of our ESVIO in the low-texture environment. Finally, in section IV, we conduct the performance comparison of our ESVIO with ORB-SLAM3 and Ultimate SLAM in offline quadrotor flight.

I. INTRODUCTION OF SELF-COLLECTED DATASET

The self-collected dataset (Table I in [1]) contains stereo event data at 60Hz and stereo image frames at 30Hz with resolution in 346×260 , as well as IMU data at 1000Hz. The timestamps between all sensors are synchronized in hardware. We also provide ground truth poses from a motion capture system VICON at 50Hz during the beginning and end of each sequence, which can be used for trajectory evaluation. To alleviate disturbance from the motion capture system's infrared light on the event camera, we add an infrared filter on the lens surface of the DAVIS346 camera. Note that this might cause the degradation of perception for both the event and image camera during the evaluation, but it can also further increase the challenge of our dataset for the only image-based method.

It is worth mentioning that this is a very challenging dataset for event-based VO/VIO, featuring aggressive motion and HDR scenarios. EVO [2], ESVO [3], Ultimate SLAM [4] are failed in most of the sequences. We think that parameter tuning is infeasible, therefore, we suggest the users use the same set of parameters during the evaluation. We hope that our dataset can help to push the boundary of future research on event-based VO/VIO algorithms, especially the ones that are really useful and can be applied in practice. For the convenience of the community, we also release the results of our methods, including the estimated 6-DoF pose and the ground truth, in the form of rosbag¹. We figure out this solution for benchmark testing and performance comparison rather than re-run our source code.

II. QUANTITATIVE EVALUATION OF OUR ESIO AND ESVIO

A. Quantitative Evaluation on rosbag

Different from the evaluated metric of the original paper, in this section, we also give the accuracy evaluation in absolute trajectory error (ATE) format. The accuracy is measured with ATE aligning the estimated trajectory with ground truth using 6-DOF transformation (in SE3), which is calculated by the tool [5]. TableI and TableII is the evaluation of our methods in self-collected dataset, Vector [6], and MVSEC [7], respectively. They are also corresponding to Table I and Table II in our original manuscript [1] respectively.

We also evaluate EVO [2] and ESVO [3] in our self-collected datasets, but they failed in all sequences. Therefore, we do not list them in TableI. This might be caused by three factors: Firstly, both EVO and ESVO have strict initialization requirements. For example, EVO requires running in a uniform scene for a few seconds to boost the system. Secondly, they are sensitive to parameter tuning, even in their open-source project, they use different parameters for different sequences in the same scenarios. We might fail to correctly tune parameters for their successful running. Finally, our dataset is so challenging that only reliable methods can perform well. As for the data sequence of MVSEC [7] and Vector [6], we list the result of EVO [2] and ESVO [3] in TableII, but they still fail in most of the sequences.

Please note that we think that parameter tuning is infeasible. Therefore, we evaluate our methods using fixed parameters for all sequences during the evaluations. We also use this criterion when evaluating other methods as a comparison. However, the generalization capability of [2] [3] is slightly poor, they need finely parameter tuning for different rosbag. We have tried our best to tune the parameter of these methods during the evaluation, however, their performance is still unsatisfactory. Meanwhile, the performance of ESVO [3] in Table II is worse than that of the original paper, which should be caused by the intercept of the time period from the original rosbag. For example, ESVO [3] only can work well during [0-27s] of sequence *Indoor Flying 3* (the total duration is 94s), but it has significant drifts after 27s. Instead, we use the whole sequence *Indoor Flying 3* without any timestamp modification. The absolute mean error of the original paper and our results are 0.19m and 0.91m respectively.

Supplementary update: We found that [8] also evaluated their method in *school-dolly* and *school-scooter* sequences. However, their video only shows the performance of their proposed method during [0-10s] of sequence *school-dolly* (the total duration is 108s) and [0-8s] of sequence *school-scooter* (the total duration is 45s). Therefore, their evaluations in these two data sequences

¹https://github.com/arclab-hku/Event_based_VO-VIO-SLAM/blob/main/Results_for_comparison.md

are not complete. Meanwhile, their algorithm cannot run in real-time and need to slow down the playback of the *rosbag*. While our ESVIO can estimate poses accurately in real-time even in high-resolution cameras.

Besides, we emphasize real-time performance when evaluating our methods, while the computational burden of EVO [2] and ESVO [3] is so large that we had to slow down the *rosbag* such as $\times 0.2$ or $\times 0.5$ data-speed, during the evaluations. Other compared methods are evaluated using the original data speed of the *rosbag*. The running time of our methods can be seen in the original manuscript. We also provide a visual comparison between our method and the other methods in the accompanying video, and all the video records of our ESVIO during the evaluations can be also obtained on our website.

We also evaluate our ESIO and ESVIO in DSEC [9] dataset, however, since the DSEC dataset does not provide the ground truth 6-DoF poses, we cannot obtain the quantitative results. Therefore, we only show the qualitative results which would be further discussed in section III-A.

TABLE I. Accuracy Comparison of Our ESVIO on HKU Dataset

Sequence	ORB-SLAM3 [10] Stereo VIO	VINS-Fusion [11] Stereo VIO	USLAM [12] Mono EIO	USLAM [4] Mono EVIO	PL-EVIO [13] Mono EVIO	Our ESIO Stereo EIO	Our ESIO+ Stereo EIO	Our ESVIO Stereo EVIO
hku_agg_translation	0.095	0.069	10.41	0.38	0.048	0.38	0.35	0.063
hku_agg_rotation	0.23	0.88	<i>failed</i>	2.06	0.15	0.87	0.51	0.11
hku_agg_flip	0.14	0.45	4.32	2.66	0.15	1.47	1.23	0.14
hku_agg_walk	<i>failed</i>	<i>failed</i>	<i>failed</i>	1.75	0.37	1.31	1.14	0.27
hku_hdr_circle	0.083	2.52	0.46	0.66	0.068	0.69	0.23	0.081
hku_hdr_slow	0.086	0.073	<i>failed</i>	1.52	0.069	0.16	0.17	0.059
hku_hdr_tran_rota	0.20	0.075	<i>failed</i>	1.74	0.068	0.55	0.60	0.065
hku_hdr_agg	0.28	1.18	<i>failed</i>	2.40	0.14	2.27	1.37	0.10
hku_dark_normal	<i>failed</i>	0.80	<i>failed</i>	2.01	1.25	0.28	0.32	0.39
Average	0.16	0.76	5.06	1.69	0.26	0.89	0.66	0.14

*EIO means purely event-based VIO, EVIO means event-based VIO with image-aided

TABLE II. Accuracy Comparison of Our ESVIO with Other Image-based or Event-based Methods

Sequence	ORB-SLAM3 [10] Stereo VIO	VINS-Fusion [11] Stereo VIO	EVO [2] Mono EO	ESVO [3] Stereo EO	Ultimate SLAM [4] Mono EVIO	PL-EVIO [13] Mono EVIO	Our ESIO Stereo EVIO	
VECtor [6]	corner-slow	0.012	0.013	0.035	0.039	0.039	0.017	0.012
	robot-normal	0.029	0.023	0.13	<i>failed</i>	0.047	0.027	0.043
	robot-fast	0.15	<i>failed</i>	<i>failed</i>	<i>failed</i>	0.35	0.037	0.042
	desk-normal	0.039	0.040	<i>failed</i>	<i>failed</i>	0.19	0.31	0.052
	desk-fast	0.099	0.10	<i>failed</i>	<i>failed</i>	0.34	0.043	0.042
	sofa-normal	0.044	0.038	<i>failed</i>	0.53	1.72	0.058	0.047
	sofa-fast	0.064	0.17	<i>failed</i>	<i>failed</i>	0.76	0.050	0.052
	mountain-normal	0.026	0.30	<i>failed</i>	<i>failed</i>	0.27	0.32	0.044
	mountain-fast	0.52	<i>failed</i>	<i>failed</i>	<i>failed</i>	1.02	0.031	0.039
	hdr-normal	0.019	0.038	<i>failed</i>	<i>failed</i>	0.17	0.12	0.017
	hdr-fast	0.040	0.055	<i>failed</i>	<i>failed</i>	0.48	0.036	0.039
	corridors-dolly	0.80	1.46	<i>failed</i>	<i>failed</i>	<i>failed</i>	1.23	0.88
	corridors-walk	1.03	0.39	<i>failed</i>	<i>failed</i>	<i>failed</i>	0.72	0.34
	school-dolly	0.92	1.79	<i>failed</i>	13.71	<i>failed</i>	3.11	0.53
	school-scooter	0.75	0.56	<i>failed</i>	9.83	6.83	1.39	0.63
MVSEC [7]	units-dolly	18.06	10.39	<i>failed</i>	<i>failed</i>	<i>failed</i>	13.82	8.12
	units-scooter	14.50	11.47	<i>failed</i>	<i>failed</i>	<i>failed</i>	11.66	6.64
	Indoor Flying 1	1.42	0.40	1.36	1.07	<i>failed</i>	0.36	0.25
	Indoor Flying 2	1.70	2.10	<i>failed</i>	1.10	<i>failed</i>	0.30	0.30
	Indoor Flying 3	1.54	0.39	1.37	0.91	<i>failed</i>	0.34	0.25
	Indoor Flying 4	0.58	0.30	<i>failed</i>	<i>failed</i>	0.23	0.44	0.46

B. Quantitative Evaluation on Onboard Quadrotor Flighting

Apart from the evaluation on *rosbag*, we also test our proposed method in the quadrotor platform. More details about this evaluation can be seen in our original manuscript [1]). We show the relative pose error (RPE) of the quadrotor flight using our ESVIO in the original manuscript. Here, we demonstrate the absolute pose error (APE) of our ESVIO compared with the ground truth in Fig.1.

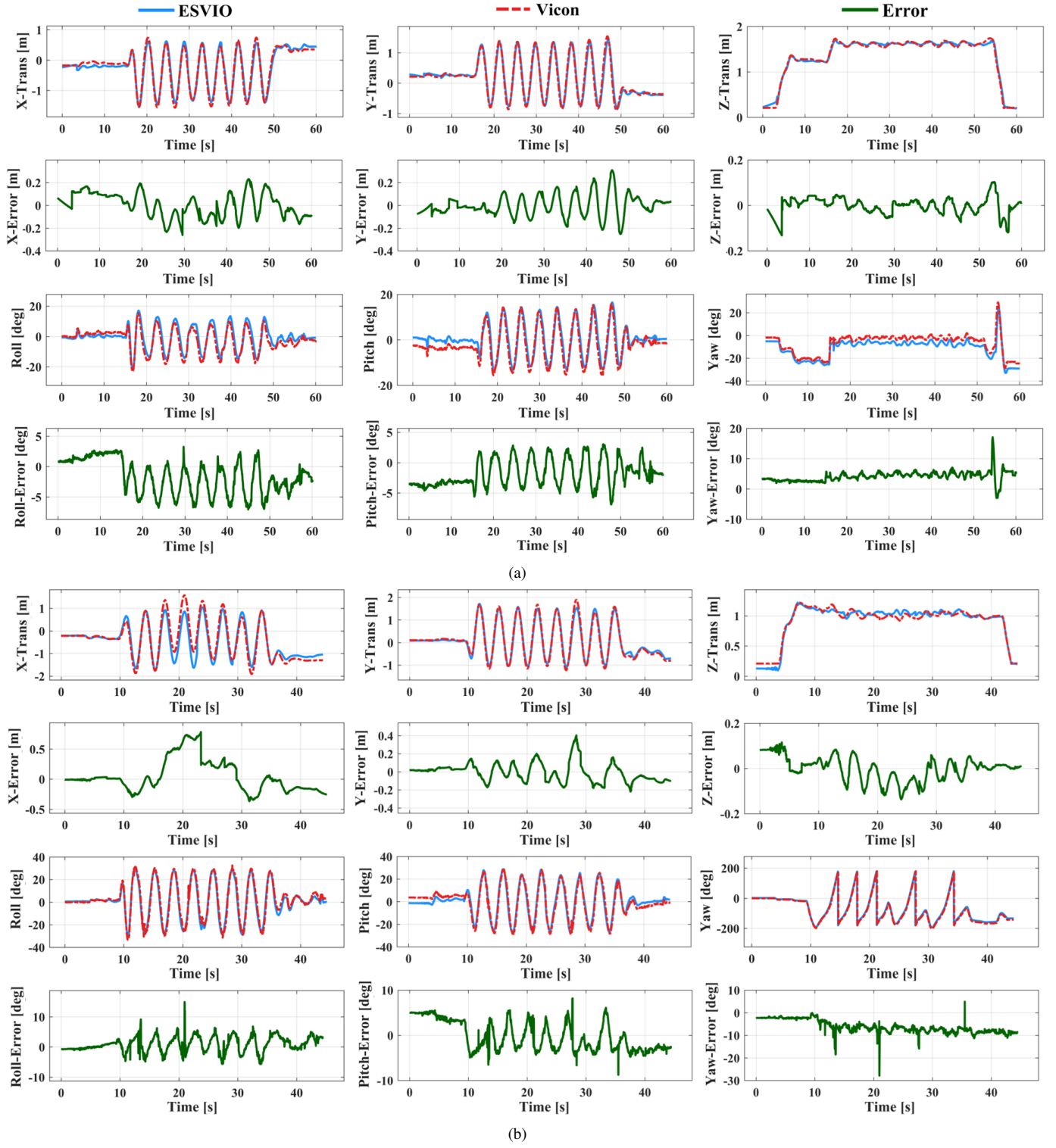


Fig. 1. The position (X, Y, Z), orientation (Roll, Pitch, Yaw), and the corresponding errors of our ESVIO compared with the VICON: (a) Onboard quadrotor flight in low-illumination conditions; (b) Onboard quadrotor flight in aggressive motion.

1) Quadrotor Flight in HDR Scenarios: We give the translational and rotational results of our ESVIO against the VICON in Fig. 1(a). The total trajectory length is 56.0m. The translation errors in the X and Y axis are within 0.3m, while the error in the Z axis is within 0.1m. For the rotational part, the error of roll and pitch are both within 6° . The error in yaw at 55s is larger than 10° , which is caused by rapid change in yaw at that moment resulting in the estimated pose being slightly slower than VICON. The root-mean-square error (RMSE) in HDR flight is 0.17m.

2) Quadrotor Flight in Aggressive Motion: In this section, the yaw angle of the commanded pattern is changed drastically, for aggressive motion. The performance of our ESVIO is quantitatively evaluated in Fig. 1(b). Note that it would have some outliers during the comparison with the VICON. For example, there is an error that is more than 10° in the roll and yaw axis at 22s. This is caused by VICON’s ball is not well observed during aggressive flight, resulting in an inaccurate measurement of the VICON at that moment. However, our reliable ESVIO state estimator still provides robust and accurate onboard pose feedback for the quadrotor. The RMSE of our ESVIO in this aggressive flight is 0.26m.

III. QUALITATIVE EVALUATION OF OUR ESIO AND ESVIO

A. Qualitative Evaluation on DSEC Dataset

To show the performance of our proposed methods in large-scale scenes, apart from outdoor large-scale HKU campus evaluation, we also perform the qualitative evaluation on the public driving dataset DSEC [9]. Since the DSEC dataset does not provide the ground-truth of the trajectory, we cannot evaluate our proposed methods quantitatively. The data sequence of DSEC was collected from stereo event cameras mounted on a driving car with 640×480 resolution. Driving scenarios are challenging for event-based sensors because forward motions typically produce considerably fewer events in the center of the image (where apparent motion is small) than in the periphery. Additionally, the higher sensor resolution (640×480), the large-scale outdoor scenes, and the dynamic objects (moving cars) are also challenging. Thanks to the robustness of our proposed method, both our ESIO (only event+IMU) and ESVIO (event+image+IMU) can perform fairly good results (shown in Fig. 2).

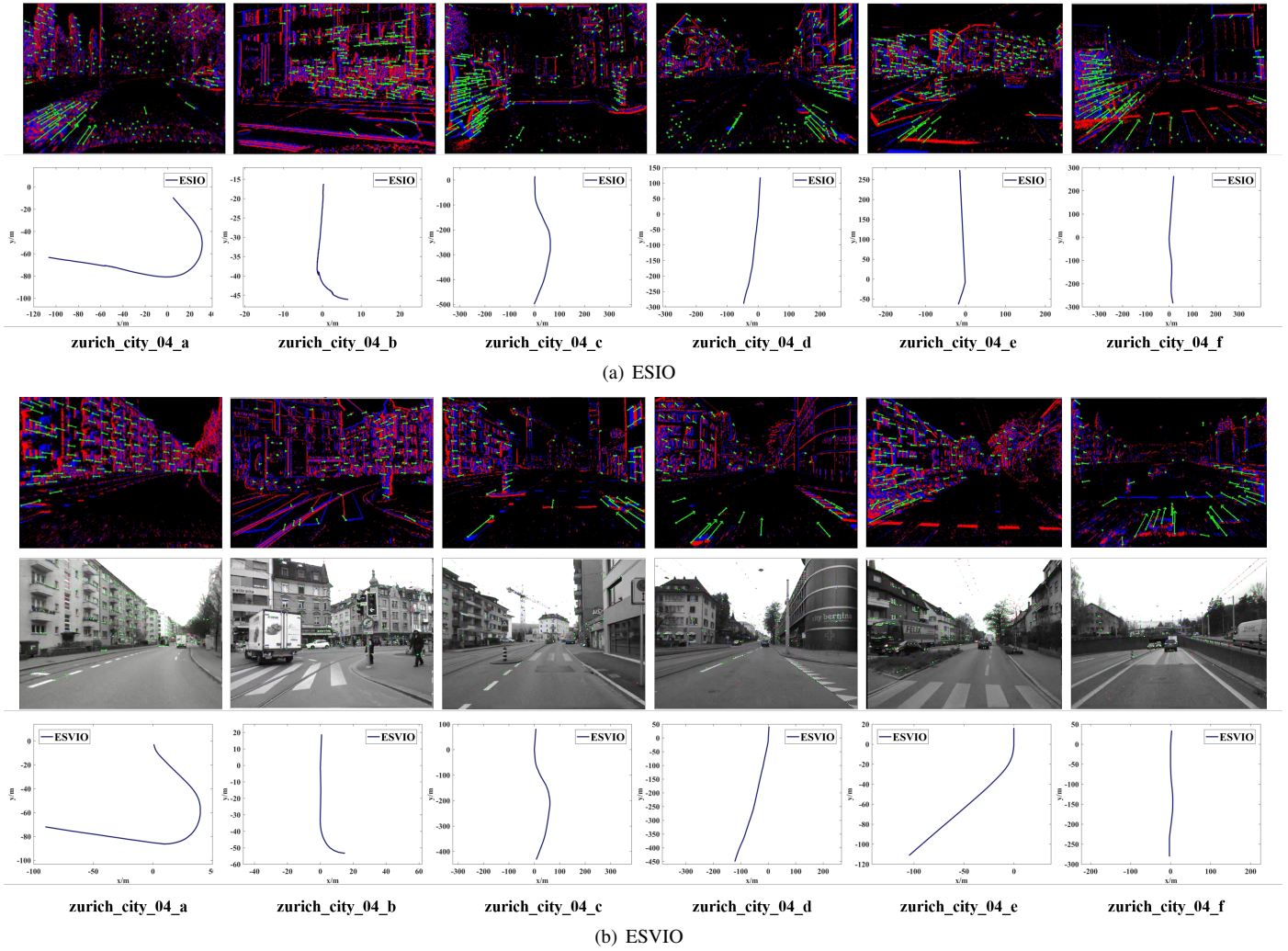


Fig. 2. Since the DSEC dataset does not provide the ground truth 6-DoF poses, we only show the qualitative results, the tracking performance of event-based and image-based features, of (a) ESIO and (b) ESVIO for the DSEC dataset sequences zurich_city_04_a to zurich_city_04_f.

Note that Ref. [3] and [14] also evaluate their method in DSEC, however, they can not run in real-time and need to slow down the playback of the rosbag. While both our ESIO and ESVIO can perform in real-time and have good results even in very heavy events load. All the evaluations of our proposed method are recorded in videos².

What's more, the data sequence of different sensors in DSEC is divided and in different data formats, which is difficult to use for VO/VIO/SLAM researchers. Therefore, we convert them into the same rosbag which might be easier for event-based VIO evaluation. The processing code and the data can be also available on our project website.

B. Qualitative Evaluation on HKU / self-collected Dataset

In this section, we visual the failure cases of ORB-SLAM3 [10], VINS-Fusion [11], and Ultimate-SLAM [4] in our self-collected data sequence. As can be seen in Table I, both our ESIO and ESVIO have good performance, especially for the sequence hku_agg_walk and hku_dark_normal, our ESVIO and ESIO still can produce reliable and accurate pose estimation even when the state-of-the-art image-based VIO method fails. As can be shown in Fig.3(a), both the ORB-SLAM3 and VINS-Fusion can not achieve reliable feature tracking under the aggressive motion due to motion blur, which causes the failure of the trajectory estimator. While our ESVIO performs satisfactory results compared with the ground truth from VICON. As for the evaluation in Fig.3(b), the ORB-SLAM3 can not extract any feature in the dark environment. As for the Ultimate SLAM, although it can detect some features in the event frame, it still cannot perform successfully feature tracking and data association in this situation. Therefore, both the ORB-SLAM3 and Ultimate SLAM fail in this case. While our proposed ESVIO can perform reliable feature detection and tracking in this harsh environment with good alignment with the ground truth.

It is worth mentioning that all the evaluations of our ESIO and ESVIO are recorded in video, which is available on our website, we refer the readers to the qualitative evaluation through consecutive videos rather than just through a single timestamp.

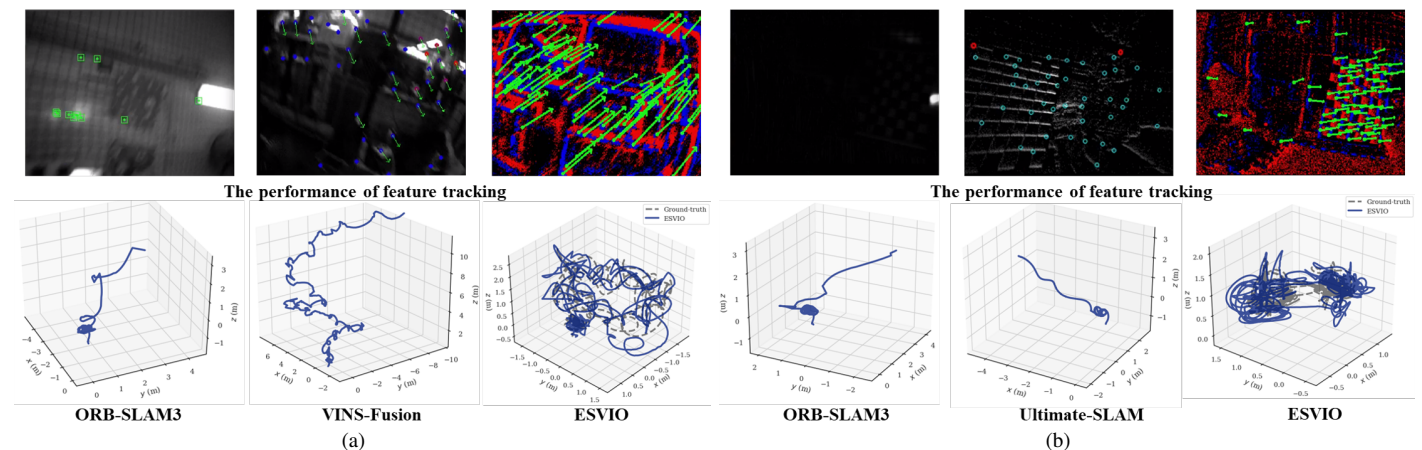


Fig. 3. The comparison of our ESVIO with ORB-SLAM3 [10], VINS-Fusion [11], and Ultimate SLAM [4] in our self-collected dataset. (a) The cases in hku_agg_walk sequences. (b) The cases in hku_dark_normal sequences.

C. Qualitative Evaluation on VECToR large-scale sequence

As can be seen in TableII, although our ESVIO achieves fairly good results compared with the state-of-the-art image-based and event-based VIO, it still has limitations in the low-texture environment. For example, the scenarios in sequence *units-dolly* and *units-scooter* are so special that the visual-only method might be easy to degenerate or mismatch during the loop-closure detection. Most of the scenes in these two sequences are low-texture, which leads to few event generations, this might cause some trouble for the methods that depend on event streams. Thanks to our well-design event-corner feature management, and the framework of the tightly-couple event, image, and IMU data fusion, our proposed ESVIO still can achieve good results compared with the ground truth in most of the sequences. However, this still indicates that either event camera or standard camera has limitations, although event cameras play a complementary role to the traditional image-based method, multi-sensor fusion, especially vision-based and non-vision-based, should be developed to exploit the complementary advantage of different sensors.

What's more, as can be seen from the video record of the evaluation using our ESVIO (take the *school-scooter*³ in Vector and *indoor_flying_1*⁴ in MVSEC [7] as examples). The estimated trajectory of our ESVIO is very smooth rather than serrate-like

²<https://b23.tv/6ByR30F>

³<https://b23.tv/pk7jdKp>

⁴<https://b23.tv/SmuzhgB>

trajectory with shaking like Ref. [3] [14] [8]. Reliable and smooth state estimation is really important in onboard perception and localization. This is also the reason that we emphasize the real-time and robust capability of our proposed methods which can not only achieve satisfactory real-time performance but also ensures the practicality and reliable onboard quadrotor flight.

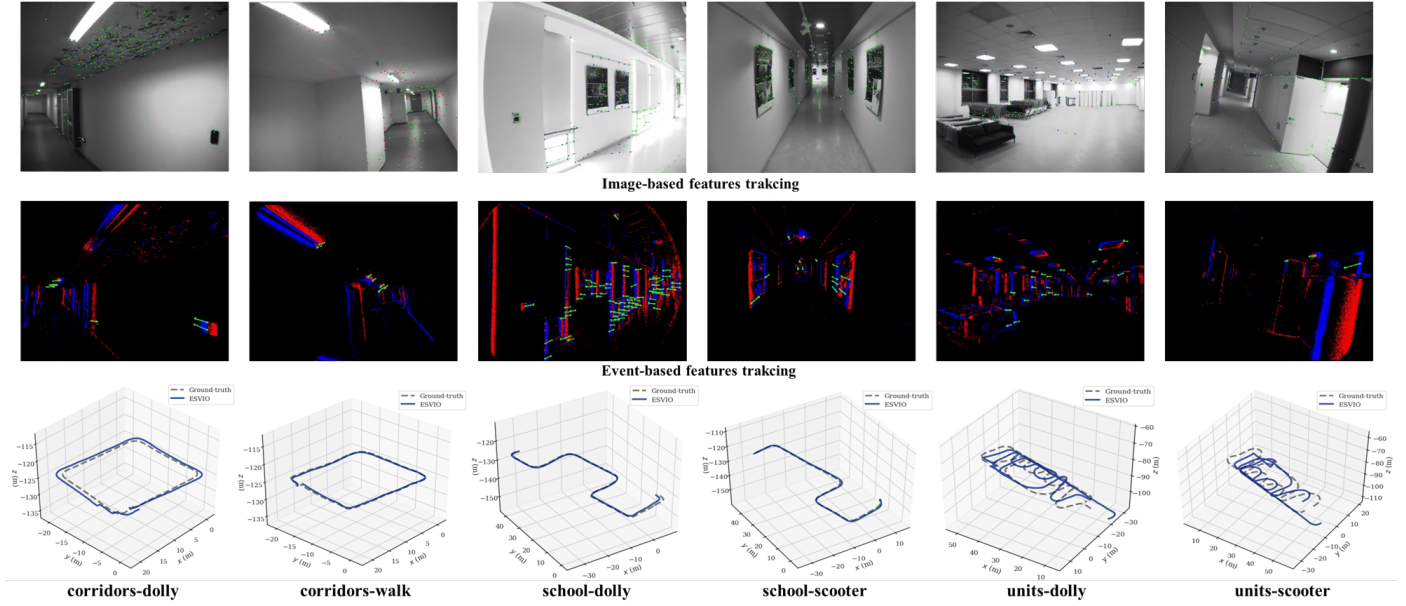


Fig. 4. Qualitative evaluation of our ESVIO in VECtor large-scale sequences. **Top:** The stereo image-based feature tracking performance; **Middle:** The stereo event-corner feature tracking performance; **Bottom:** The estimated trajectories produced by our ESVIO.

IV. PERFORMANCE COMPARISON ON HDR OFFLINE QUADROTOR FLIGHT

In [1], we only demonstrate that using our ESVIO for onboard quadrotor flight. In this section, we conduct a new experiment that records the sensor data during quadrotor flight and then use it to compare the performance of our ESVIO, ORB-SLAM3 [10], and Ultimate SLAM [4]. Similar to [1], the state estimation from our ESVIO is used to provide onboard pose feedback control for the quadrotor. The quadrotor is commanded to follow a circular pattern eight times continuously during the experiment. The robust and accurate onboard state estimates of our ESVIO enable real-time feedback control. We record the rosbag which includes the ground truth from VICON, stereo event stream, stereo image, and IMU, for evaluation. As can be seen from the top two rows of Fig.5, in the condition of turning off the light, all the image-based features tracking is unreliable and rare in these three methods. However, thanks to our robust and reliable stereo event-corner feature detection and association, only our ESVIO can perform reliable and accurate state estimation. While both ORB-SLAM3 and Ultimate SLAM failed in the HDR quadrotor flight. The comparison of our ESVIO with other SOTA algorithms can be seen in the video⁵.

REFERENCES

- [1] P. Chen, W. Guan, and P. Lu, “Esvio: Event-based stereo visual inertial odometry,” *arXiv preprint arXiv:2212.13184*, 2022.
- [2] H. Rebecq, T. Horstschäfer, G. Gallego, and D. Scaramuzza, “Evo: A geometric approach to event-based 6-dof parallel tracking and mapping in real time,” *IEEE Robotics and Automation Letters*, vol. 2, no. 2, pp. 593–600, 2017.
- [3] Y. Zhou, G. Gallego, and S. Shen, “Event-based stereo visual odometry,” *IEEE Transactions on Robotics*, 2021.
- [4] A. R. Vidal, H. Rebecq, T. Horstschaefer, and D. Scaramuzza, “Ultimate slam? combining events, images, and imu for robust visual slam in hdr and high-speed scenarios,” *IEEE Robotics and Automation Letters*, vol. 3, no. 2, pp. 994–1001, 2018.
- [5] M. Grupp, “evo: Python package for the evaluation of odometry and slam,” *Note: https://github.com/MichaelGrupp/evo Cited by: Table*, vol. 7, 2017.
- [6] L. Gao, Y. Liang, J. Yang, S. Wu, C. Wang, J. Chen, and L. Kneip, “Vector: A versatile event-centric benchmark for multi-sensor slam,” *IEEE Robotics and Automation Letters*, 2022.
- [7] A. Z. Zhu, D. Thakur, T. Özaslan, B. Pfommer, V. Kumar, and K. Daniilidis, “The multivehicle stereo event camera dataset: An event camera dataset for 3d perception,” *IEEE Robotics and Automation Letters*, vol. 3, no. 3, pp. 2032–2039, 2018.
- [8] K. Wang and K. Zhao, “Stereo event-based visual-inertial odometry,” *arXiv preprint arXiv:2303.05086*, 2023.
- [9] M. Gehrig, W. Aarents, D. Gehrig, and D. Scaramuzza, “Dsec: A stereo event camera dataset for driving scenarios,” *IEEE Robotics and Automation Letters*, vol. 6, no. 3, pp. 4947–4954, 2021.
- [10] C. Campos, R. Elvira, J. J. G. Rodríguez, J. M. Montiel, and J. D. Tardós, “Orb-slam3: An accurate open-source library for visual, visual–inertial, and multimodal slam,” *IEEE Transactions on Robotics*, 2021.

⁵<https://b23.tv/ExrSI3M>

- [11] T. Qin, J. Pan, S. Cao, and S. Shen, "A general optimization-based framework for local odometry estimation with multiple sensors," *arXiv preprint arXiv:1901.03638*, 2019.
- [12] H. Rebecq, T. Horstschaefer, and D. Scaramuzza, "Real-time visual-inertial odometry for event cameras using keyframe-based nonlinear optimization," in *British Machine Vision Conference (BMVC)*, 2017.
- [13] W. Guan, P. Chen, Y. Xie, and P. Lu, "Pi-evio: Robust monocular event-based visual inertial odometry with point and line features," *arXiv preprint arXiv:2209.12160*, 2022.
- [14] Z. Liu, D. Shi, R. Li, and S. Yang, "Esvio: Event-based stereo visual-inertial odometry," *Sensors*, vol. 23, no. 4, p. 1998, 2023.

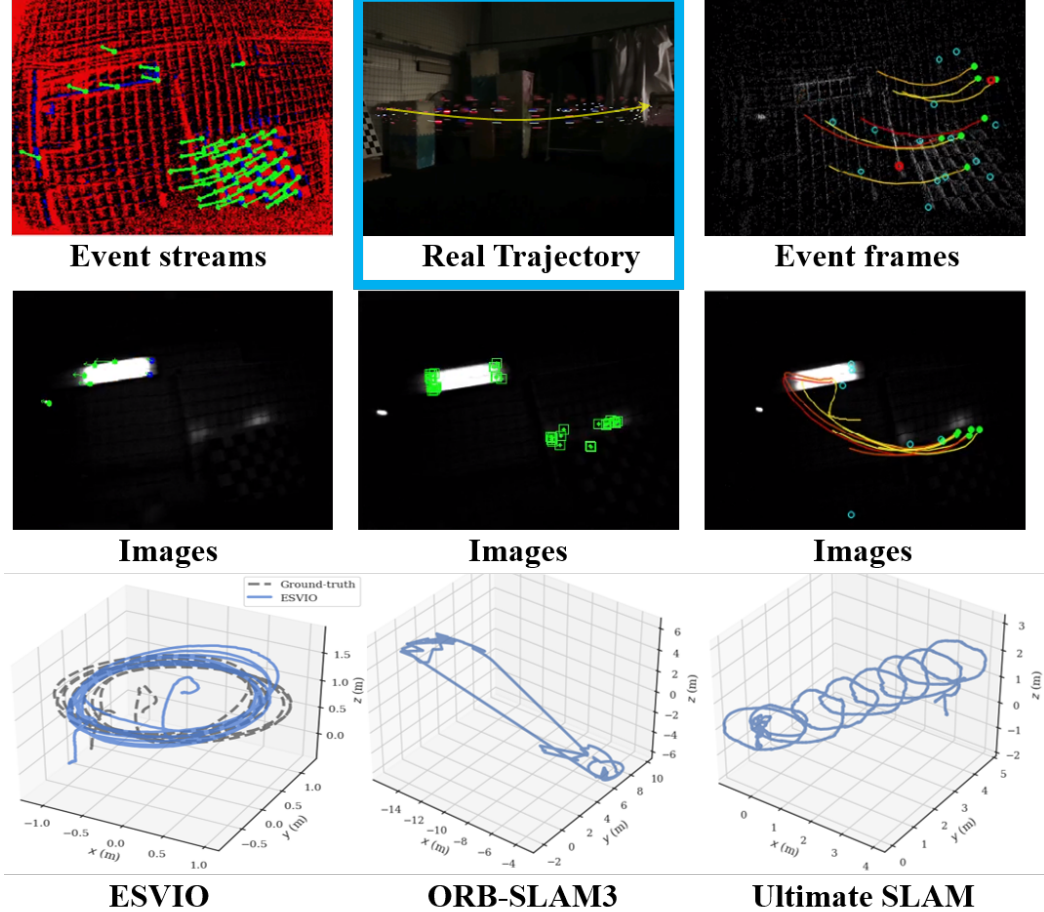


Fig. 5. Performance comparison of our ESVIO with ORB-SLAM3 and Ultimate SLAM in HDR offline quadrotor flight